MARTINI: An event generator for relativistic heavy-ion collisions

Björn Schenke, Charles Gale, and Sangyong Jeon
Department of Physics, McGill University, Montreal, Quebec, H3A 2T8, Canada
(Received 23 October 2009; published 30 November 2009)

We introduce the modular algorithm for relativistic treatment of heavy ion interactions (MARTINI), a comprehensive event generator for the hard and penetrating probes in high-energy nucleus-nucleus collisions. Its main components are a time-evolution model for the soft background, PYTHIA 8.1, and the McGill-Arnold, Moore, and Yaffe (AMY) parton-evolution scheme, including radiative as well as elastic processes. This allows us to generate full event configurations in the high p_T region that take into account thermal quantum chromodynamic (QCD) and quantum electrodynamic (QED) effects as well as effects of the evolving medium. We present results for the neutral pion nuclear modification factor in Au + Au collisions at the BNL Relativistic Heavy Ion Collider as a function of p_T for different centralities and also as a function of the angle with respect to the reaction plane for noncentral collisions. Furthermore, we study the production of high-transverse-momentum photons, incorporating a complete set of photon-production channels.

DOI: 10.1103/PhysRevC.80.054913 PACS number(s): 24.85.+p, 25.75.−q, 12.38.Mh

I. INTRODUCTION

High-transverse-momentum jets emerging from the central rapidity region in heavy-ion collisions provide important information on the produced hot quark-gluon plasma (QGP). To extract this information from the experimental data, it is important to develop a good theoretical understanding of the interactions of hard partons with the medium. Therefore, the energy loss of hard partons traversing the medium has been under extensive theoretical investigation. Gluon bremsstrahlung, including the Landau-Pomeranchuk-Migdal (LPM) [1] effect, has been proposed as the dominant mechanism for energy loss, and different theoretical formalisms have been developed and applied to describe it [2–12]. Also, binary elastic scattering of thermal partons is potentially important for the energy loss and momentum broadening of high-p_T partons. In Ref. [13], elastic energy loss was combined with the Arnold, Moore, and Yaffe (AMY) [10–12] radiative energy loss within the McGill-AMY evolution formalism, and in Ref. [14] the description of the collision processes was further improved.

The main goal of these and other calculations is to create a quantitative basis for the "tomography" of the hot and dense nuclear medium created in heavy-ion collisions. Among the tomographic variables is the nuclear modification factor R_{AA}, which is defined as the ratio of the hadron yield in A + A collisions to that in binary-scaled $p + p$ interactions. A variety of computations that differ significantly in the applied-energy-loss mechanism can reproduce the measured R_{AA} in central Au + Au collisions at $\sqrt{s} = 200A$ GeV at the Relativistic Heavy-Ion Collider (RHIC), given the present experimental errors. (See Ref. [15] for a systematic comparison of three different formalisms.) For this reason, the tomographic usefulness of R_{AA} in central collisions has become questionable [16]. More differential observables, such as R_{AA} as a function of both p_T and azimuth in noncentral collisions [17–20], can help to improve this situation.

Other important observables in heavy-ion collisions are electromagnetic probes, such as photons and dileptons. Because of the small electromagnetic coupling, once produced, they usually escape the medium without further interaction and thus provide undistorted information on the early stages of a heavy-ion collision. Photon production from nuclear collisions at RHIC has been calculated in Refs. [21–23] using (1 + 1)-dimensional Bjorken evolution, (2 + 1)-dimensional, or (3 + 1)-dimensional relativistic hydrodynamic evolution for the background, respectively. Photons in nuclear collisions come from a variety of sources, namely direct photons, fragmentation photons, jet-plasma photons, and thermal photons. Direct photons are predominantly produced from hard collisions in the early stage of the heavy-ion collision via annihilation and the Compton scattering processes. Fragmentation photons are produced from the surviving high-energy jets after their passing through the thermal medium. Thermal photons have a negligible contribution at high p_T and thus are not relevant in this range. However, jet-plasma photons from photon radiation $q \to q\gamma$ (bremsstrahlung photons) and jet-photon conversion via Compton and annihilation processes have been shown to be very important for the understanding of experimental data for photon production in Au + Au collisions at RHIC [21–24].

For the best possible comparison of the theoretical description with experimental data, we incorporate the McGill-AMY formalism [10–13,25] for radiative energy loss as well as elastic processes [14] into a new event generator, dubbed modular algorithm for relativistic treatment of heavy ion interactions (MARTINI). Its main ingredients are PYTHIA 8.1 [26,27] to generate the hard partons from the individual nucleon-nucleon collisions and to take care of the final fragmentation into hadrons, the evolution of the background medium (e.g., from hydrodynamic models), and the McGill-AMY parton-evolution formalism. This way, it is possible to study hard observables in heavy-ion collisions theoretically on an event-by-event basis, keeping information on correlations.

Several Monte Carlo simulations for heavy-ion collisions have been or are being developed [28–36]. The implementation of medium effects and use of approximations varies significantly between the different models. MARTINI is the first Monte Carlo simulation to include AMY bremsstrahlung combined

with elastic processes and in-medium photon production. It is very flexible because of its ability to incorporate any soft background evolution that provides information on the temperature and flow velocities of the medium. Currently, hydrodynamic evolution calculations from four different groups [37–42] have been implemented.

In this work, we present the first results on hard observables obtained with MARTINI. These include the azimuth-averaged $R_{\rm AA}$ as a function of p_T, $R_{\rm AA}$ as a function of the azimuth and p_T, as well as photon yields and photon $R_{\rm AA}$.

This article is organized as follows. We review the McGill-AMY evolution formalism and present transition rates for radiative and elastic processes in Sec. II. We introduce the Monte Carlo simulation in Sec. III, present our results in Sec. IV, and conclude and present an outlook in Sec. V.

II. McGILL-AMY EVOLUTION FORMALISM

At the core of MARTINI lies the McGill-AMY formalism for jet evolution in a dynamical thermal medium. Here, we briefly review this formalism and discuss its implementation into MARTINI in the following section.

In previous works [13,23,25], the evolution of the jet-momentum distribution in a hydrodynamic background was computed within the McGill-AMY scheme. This evolution is governed by a set of coupled Fokker-Planck-type rate equations of the form

$$\frac{dP(p)}{dt} = \int_{-\infty}^{\infty} dk \left[P(p+k)\frac{d\Gamma(p+k,k)}{dk} - P(p)\frac{d\Gamma(p,k)}{dk}\right], \tag{1}$$

where $d\Gamma(p,k)/dk$ is the transition rate for processes where partons of energy p lose energy k. The $k<0$ part of the integration incorporates processes that increase a parton's energy.

In the approach of the AMY finite-temperature-field theory, the energy loss of hard partons is considered in a medium at an asymptotically high temperature so that the QCD coupling is weak. In this regime, an analytical treatment is possible, and a hierarchy of parametrically separated scales ($T \gg gT \gg g^2T$) emerges. This allows radiative transition rates to be calculated by means of integral equations [12], which correctly reproduce both the Bethe-Heitler and the LPM results in their respective limits. They are given by [21,43]:

$$\frac{d\Gamma}{dk}(p,k) = \frac{C_s g^2}{16\pi p^7}\frac{1}{1\pm e^{-k/T}}\frac{1}{1\pm e^{-(p-k)/T}} \times \begin{Bmatrix} \frac{1+(1-x)^2}{x^3(1-x)^2}, & q\to qg, \\ N_f\frac{x^2+(1-x)^2}{x^2(1-x)^2}, & g\to q\bar{q}, \\ \frac{1+x^4+(1-x)^4}{x^3(1-x)^3}, & g\to gg \end{Bmatrix} \times \int \frac{d^2\mathbf{h}}{(2\pi)^2} 2\mathbf{h}\cdot \mathrm{Re}\,\mathbf{F}(\mathbf{h},p,k), \tag{2}$$

where g is the strong coupling constant [$\alpha_s = g^2/(4\pi)$], N_f is the number of flavors, C_s is the quadratic Casimir relevant for the process, and $x \equiv k/p$ is the momentum fraction of the radiated gluon (or the quark, for the case $g\to q\bar{q}$). The relation $\mathbf{h} \equiv (\mathbf{k}\times\mathbf{p})\times\mathbf{e}_\parallel$ determines how noncollinear the final state is, where $\mathbf{e}_\parallel$ is the unit vector in a direction nearly collinear with $\mathbf{k}$, $\mathbf{p}$, and $\mathbf{p}+\mathbf{k}$, which can be fixed by convention (see Ref. [12]). Parametrically $\mathbf{h}$ is of order gT^2 and hence is small compared to $\mathbf{p}\cdot\mathbf{k}$. Therefore, $\mathbf{h}$ can be taken as a two-dimensional vector in transverse space. $\mathbf{F}(\mathbf{h},p,k)$ is the solution of the following integral equation [21,43]:

$$\begin{aligned} 2\mathbf{h} = {} & i\delta E(\mathbf{h},p,k)\mathbf{F}(\mathbf{h}) + g_s^2\int\frac{d^2\mathbf{q}_\perp}{(2\pi)^2}C(\mathbf{q}_\perp)\{(C_s-C_{\rm A}/2) \\ & \times[\mathbf{F}(\mathbf{h})-\mathbf{F}(\mathbf{h}-k\,\mathbf{q}_\perp)] + (C_{\rm A}/2)[\mathbf{F}(\mathbf{h})-\mathbf{F}(\mathbf{h}+p\,\mathbf{q}_\perp)] \\ & + (C_{\rm A}/2)[\mathbf{F}(\mathbf{h})-\mathbf{F}(\mathbf{h}-(p-k)\,\mathbf{q}_\perp)]\}. \end{aligned} \tag{3}$$

Here, $\delta E(\mathbf{h},p,k)$ is the energy difference between the final and the initial states,

$$\delta E(\mathbf{h},p,k) = \frac{\mathbf{h}^2}{2pk(p-k)} + \frac{m_k^2}{2k} + \frac{m_{p-k}^2}{2(p-k)} - \frac{m_p^2}{2p}, \tag{4}$$

and m^2 are the medium-induced thermal masses. $C(\mathbf{q}_\perp)$ is the differential rate to exchange transverse (to the $\parallel$ direction) momentum $\mathbf{q}_\perp$. In a hot thermal medium, its value at leading order in $\alpha_{\rm s}$ is [44]

$$C(\mathbf{q}_\perp) = \frac{m_D^2}{\mathbf{q}_\perp^2(\mathbf{q}_\perp^2+m_D^2)}, \qquad m_D^2 = \frac{g_s^2T^2}{6}(2N_{\rm c}+N_f). \tag{5}$$

For the case of $g\to q\bar{q}$, $(C_s - C_A/2)$ should appear as the prefactor on the term containing $\mathbf{F}(\mathbf{h}-p\,\mathbf{q}_\perp)$ rather than $\mathbf{F}(\mathbf{h}-k\,\mathbf{q}_\perp)$.

Transition rates for elastic processes can also be computed in perturbative QCD. They are given by [14]

$$\begin{aligned} \frac{d\Gamma}{d\omega}(p,\omega,T) = {} & d_q\int\frac{d^3q}{(2\pi)^3}\int\frac{d^3q'}{(2\pi)^3}\frac{2\pi}{16pp'qq'} \\ & \times\delta(p-p'-\omega)\delta(q'-q-\omega) \\ & \times|\mathcal{M}|^2 f(q,T)(1\pm f(q',T)), \end{aligned} \tag{6}$$

where $p=|\mathbf{p}|$ and $p'=|\mathbf{p}'|$ are the absolute values of the three-momentum of the incoming and outgoing hard partons, respectively, and $q=|\mathbf{q}|$ and $q'=|\mathbf{q}'|$ are those of the incoming and outgoing thermal partons. Then, $\omega = p-p' = q'-q$ is the transferred energy. The distribution functions f are either Fermi-Dirac or Bose-Einstein distributions, depending on the nature of the thermal parton involved. The $+$ or $-$ sign appears accordingly, with $-$ for Pauli blocking and $+$ for Bose enhancement, and d_q describes the degeneracy of the thermal parton. Integrations over q and q' in Eq. (6) can be rewritten in terms of the transferred momentum k. Then, an appropriate separation of the regimes of soft and hard momentum exchange and a hard thermal loop resummation in the soft regime to cure the infrared divergence allows for a numerical evaluation of Eq. (6). It is even possible to extend the expression for the soft regime to all momenta [14,45], which leads to a good approximation of the total result and avoids the introduction of an intermediate scale. The transition rate as a function of both the transferred energy and momentum $d\Gamma/d\omega\,dk$ is obtained

from Eq. (6) after rewriting and omitting the integration over the transferred momentum k. Using $d\Gamma/d\omega\, dk$ allows us to sample both the transferred energy and the transferred three-momentum in an elastic process.

Both radiative and elastic transition rates were computed and tabulated as functions of the parton energy p, as well as the radiated energy k or transferred energy ω and momentum k, respectively, and are sampled within MARTINI. Note that because the radiated partons are on-shell, $\omega = k$, whereas the transferred parton in an elastic collision can be far off-shell, and so ω and k are treated separately. In contrast to the radiative transition rates, the dependence on the coupling of the elastic rates is nontrivial, and the rates are also tabulated as functions of the coupling α_s.

Apart from these processes, we include gluon-quark and quark-gluon conversion due to Compton and annihilation processes, as well as the QED processes of photon radiation $q \to q\gamma$ and jet-photon conversion. The transition rate for the photon radiation process is calculated analogously to the gluon radiation [10,12], and in the limit $E \gg T$ the transition rate for quark-photon conversion is given by

$$\frac{d\Gamma^{\text{conv}}_{q\to\gamma}}{d\omega}(E,\omega) = \left(\frac{e_f}{e}\right)^2 \frac{2\pi\alpha_e\alpha_s T^2}{3E} \times \left(\frac{1}{2}\ln\frac{ET}{m_q^2} - 0.36149\right)\delta(\omega), \tag{7}$$

where m_q is the thermal quark mass, $m_q^2 = g^2T^2/6$, e_f is the charge of a quark with flavor f, α_e is the fine structure constant, and the δ function indicates that we neglect the energy loss of the quark during the process of conversion. The conversion rate $d\Gamma^{\text{conv}}_{q\to g}/d\omega$ is equal to that in Eq. (7) multiplied by a color factor $C_F = 4/3$, and

$$\frac{d\Gamma^{\text{conv}}_{g\to q}}{d\omega} = N_f \frac{N_c}{N_c^2 - 1}\frac{d\Gamma^{\text{conv}}_{q\to g}}{d\omega}, \tag{8}$$

which follows from interchanging the initial with the final jet.

III. MONTE CARLO SIMULATION

MARTINI solves the rate equations (1) using Monte Carlo methods. Instead of evolving a probability distribution $P(p)$, every event and every hard parton is treated individually. In this way, we obtain information on the full microscopic event configuration in the high-momentum regime, including correlations, which allows for a very detailed analysis and offers a direct interface between theory and experiment. The average over a large number of events corresponds to the solution found by solving Eq. (1) for the probability distribution.

We follow the evolution of one event to describe the basic functionality of the simulation. First, the number of individual nucleon-nucleon collisions that produce partons with a certain minimal transverse momentum $p_T^{\min}$ is determined from the total inelastic cross section provided by PYTHIA. The initial transverse positions $\mathbf{r}_\perp$ of these collisions are determined by the initial jet-density distribution $\mathcal{P}_{AB}(b, \mathbf{r}_\perp)$, which for A + B collisions with impact parameter $\mathbf{b}$ is given by

$$\mathcal{P}_{AB}(b, \mathbf{r}_\perp) = \frac{T_A(\mathbf{r}_\perp + \mathbf{b}/2)T_B(\mathbf{r}_\perp - \mathbf{b}/2)}{T_{AB}(b)}. \tag{9}$$

Here we use a Woods-Saxon form for the nuclear-density function, $\rho(\mathbf{r}_\perp, z) = \rho_0/[1 + \exp[(r - R)/d]$, to evaluate the nuclear thickness function, $T_A(\mathbf{r}_\perp) = \int dz \rho_A(\mathbf{r}_\perp, z)$, and the overlap function of two nuclei, $T_{AB}(b) = \int d^2r_\perp T_A(\mathbf{r}_\perp)T_B(\mathbf{r}_\perp + \mathbf{b})$. The values of the parameters $R = 6.38$ fm and $d = 0.535$ fm are taken from Ref. [46]. The initial parton-distribution functions can be selected with the help of the Les Houches Accord PDF Interface (LHAPDF) [47]. We include nuclear effects on the parton-distribution functions using the EKS98 [48] or EPS08 [49] parametrization, by user choice. In practice, we sample the initial positions of nucleons in nuclei A and B, superimpose the transverse areas depending on the impact parameter, and then divide the overlap region into circles with area σ_{inel}. In three dimensions, these are tubes, and we determine how many jet events with given $p_T^{\min}$ occur within such a tube using the number of nucleons from A and B in the tube and the probability for a jet event $\sigma_{\text{jet}}(p_T^{\min})/\sigma_{\text{inel}}$ for each of their combinations.

The soft medium is described by hydrodynamics or other models, which provide information on the system's local temperature and flow velocity $\boldsymbol{\beta}$. Before this medium has formed [i.e., before the hydrodynamic evolution begins ($\tau < \tau_0$)], the partons shower as in a vacuum. Currently, we include the complete vacuum shower, because there is no apparent reason why the vacuum splittings should end immediately once the medium has formed. Because most of the vacuum shower occurs before the medium has formed, this is a reasonable approximation. We have also tested the other extreme case where we stop the vacuum evolution at the virtuality scale $Q_{\min} = \sqrt{p_T/\tau_0}$, determined by the time τ_0 at which the medium evolution begins. This modifies the parton distribution such that the strong coupling constant has to be chosen as approximately 10% larger to describe the pion R_{AA}. At this stage, we do not include final-state radiation (FSR) of the partons that have left the medium—all vacuum showers take place before the medium evolution, and there is no interference between the medium and vacuum showers. The improvement of this point is the subject of future work. Once $\tau > \tau_0$ for a certain parton, its in-medium evolution begins. The partons move through the background according to their velocity. To compute probabilities for any one of these in-medium processes, we perform a Lorentz boost into the rest frame of the fluid cell at the parton's position and determine the transition rates according to the local temperature and the parton's energy in this local rest frame. The probability for a parton to undergo any process during a time step of length Δt is given by $\Delta t\, \Gamma(p, T)_{\text{total}}$, where $\Gamma(p, T)_{\text{total}} = \int dk d\Gamma_{\text{total}}/dk$ for the radiative processes, and the integral over both ω and k for the elastic processes. Then, $d\Gamma_{\text{total}}/dk$ is the sum over all possible transition rates, which include those for photon production.

In case some process occurs, we decide which one it is according to the relative weights of the different processes at the given temperature and parton energy. We sample the radiated or transferred energy from the transition rate of the

occurring process using the rejection method. In the case of an elastic process, we also sample the transferred transverse momentum, whereas for radiative processes we assume collinear emission for now, which is a good approximation in the weak coupling limit because the emission angle is of order g [12]. After energy and momentum are transferred, we boost back into the laboratory frame, where the parton continues to move along its trajectory. Radiated partons are also further evolved if their momentum is greater than a certain threshold $p_{\min}$, which can be set (typically we choose $p_{\min} \simeq 3$ GeV). This leads to a growing and broadening in-medium shower. The overall evolution of a parton stops once its energy in a fluid cell's rest frame is less than the limit of $4T$, where T is the local temperature. Because both radiative and elastic transition rates are computed in the limit $E \gg T$, it would not make sense to attempt to learn anything about the evolution of partons with $E \simeq T$ within this formalism. For partons that stay above that threshold, the evolution ends once they enter the hadronic phase of the background medium. In the mixed phase, processes occur only for the QGP fraction.

When all partons have left the QGP phase, hadronization is performed by PYTHIA, to which the complete information on all final partons is passed. Because PYTHIA uses the Lund string fragmentation model [51,52], it is essential to keep track of all color strings during the in-medium evolution. This includes generating new strings when a gluon is emitted or during a conversion process. In the latter case, new string ends have to be attached to thermal partons, whose momenta are sampled from Fermi or Bose distributions. Being provided with such consistent information on the color string structure, PYTHIA is able to perform the fragmentation. This concludes the evolution of one event.

The concept of MARTINI is modular, such that we can turn on and off different processes independently and use different hydrodynamic or other data inputs. In principle, it is also possible to extend MARTINI to use different energy-loss formalisms. The parameters are set using the same interface as PYTHIA, and all options for PYTHIA can still be modified by the user.

IV. RESULTS

A. Pion production and nuclear modification factor $\pi^0 R_{AA}(p_T)$

We begin by showing the MARTINI results for the spectrum of neutral pions in $p + p$ collisions at RHIC energy ($\sqrt{s} =$ 200 GeV) as well as in central (0–10%) Au + Au collisions compared to data by PHENIX [18,50] in Fig. 1. The calculations were performed using CTEQ5L parton distribution functions [53], including nuclear-shadowing effects using the EKS98 parametrization [48]. In the results shown for pion production, isospin effects were ignored. We checked that they have no big effect (less than 5%); however, we included them in calculations of photon production where they become important (15–20%). Au + Au calculations take into account both radiative and elastic processes in the medium described by either the $(2 + 1)$-dimensional hydrodynamics of [38–40] or the $(3 + 1)$-dimensional hydrodynamics of [41], using coupling constants $\alpha_s = 0.33$ or $\alpha_s = 0.3$, respectively. The α_s was adjusted to describe the experimental measurement of the

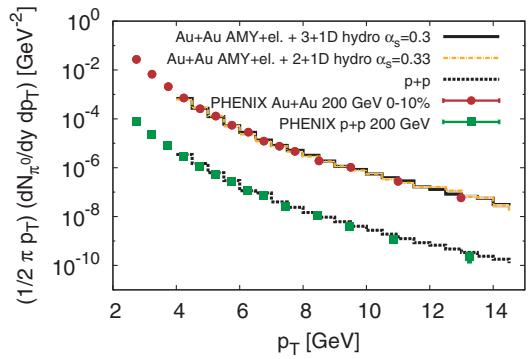

FIG. 1. (Color online) Neutral pion spectrum in $p + p$ and 0–10% central Au + Au collisions at RHIC energy compared to data by PHENIX [18,50].

neutral pion nuclear modification factor R_{AA} in most central collisions (see later sections). For both hydro evolutions $\tau_0 =$ 0.6 fm/c, PYTHIA parameters were tuned to fit the $p + p$ data; however there is still freedom, and possibly an even better set of parameters can be found. Using the same PYTHIA settings, we find very good agreement for both $p + p$ and Au + Au spectra. Note that to achieve better statistics, we used certain cutoffs for the minimal p_T produced in a nucleon-nucleon collision in PYTHIA for the Au + Au calculation. The shown result is a combination of runs with minimal $p_T^{\min} = 1.5$ GeV for $p_T \leqslant 5.5$ GeV, $p_T^{\min} = 2$ GeV for $5.5 \leqslant p_T \leqslant 6.5$ GeV, and $p_T^{\min} = 4$ GeV above that. Note that the shown results are averages over typically $\sim 5 \cdot 10^8$ simulated events.

In Fig. 2, we present the results for the neutral pion nuclear modification factor, defined by

$$R_{AA} = \frac{1}{N_{\text{coll}}(b)} \frac{dN_{AA}(b)/d^2 p_T dy}{dN_{pp}/d^2 p_T dy}, \tag{10}$$

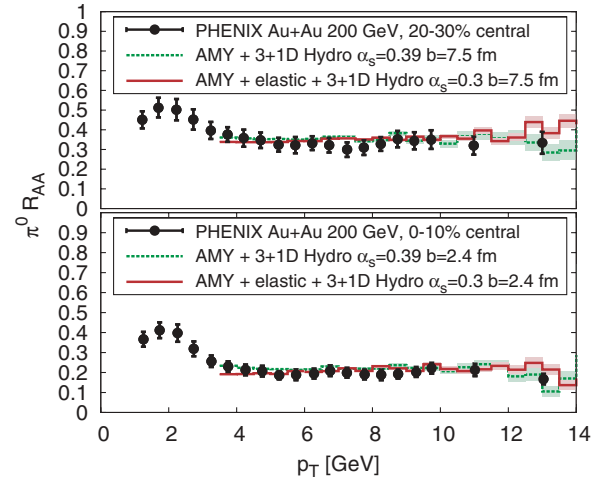

FIG. 2. (Color online) Neutral pion nuclear modification factor for midcentral (upper panel) and central (lower panel) collisions at RHIC with $\sqrt{s} = 200$ GeV. MARTINI results ($b = 2.4$ fm and $b = 7.5$ fm) using $(3 + 1)$-dimensional hydro evolution [41] and only radiative processes (dashed lines) and both radiative and elastic processes (solid lines) with different α_s are compared to PHENIX data from Ref. [54].

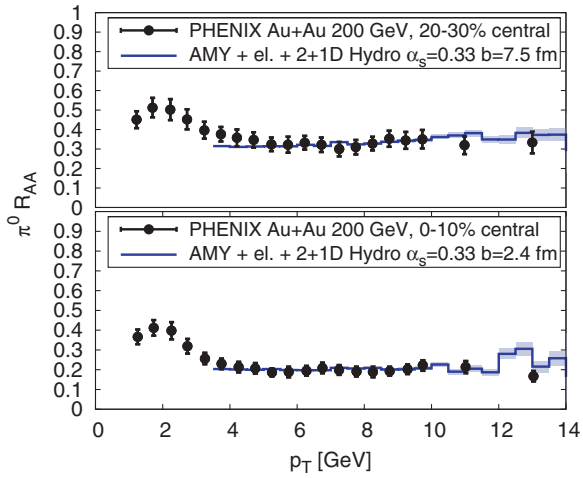

FIG. 3. (Color online) Neutral pion nuclear modification factor for midcentral (upper panel) and central (lower panel) collisions at RHIC with $\sqrt{s} = 200$ GeV. MARTINI results ($b = 2.4$ fm and $b = 7.5$ fm) using $(2 + 1)$-dimensional hydro evolution [38–40] and both radiative and elastic processes compared to PHENIX data [54].

in Au + Au collisions at RHIC measured at midrapidity in two different centrality classes (0–10% and 20–30%), employing the corresponding average impact parameters, 2.4 and 7.5 fm. We compare with the experimental measurements by PHENIX [54]. All parameters are the same as in the calculation shown in Fig. 1, that is, hydrodynamic background evolution from Ref. [41] and $\alpha_s = 0.3$. The same value of α_s is used in all following calculations. (There are no additional parameters for the calculation of the azimuthal dependence of R_{AA} or the high-p_T photon production.) We find very good agreement with the data for both centrality classes.

The value for α_s for which the data are described if we only include radiative processes is $\alpha_s \simeq 0.39$, greater than for the calculations in Ref. [13], where it was 0.33. Differences in the treatment of vacuum showers and the fragmentation scheme are responsible for this difference. We have observed that when varying parameters in PYTHIA, such as the factorization or renormalization scale, or parameters in the fragmentation function, we need slighty different α_s to describe the data. This freedom leads to an approximately 10–20% uncertainty in α_s. The value of α_s is again closer to that used in Ref. [13] ($\alpha_s = 0.27$) when including elastic processes, because the elastic energy loss in our formulation is slightly larger than that implemented in Ref. [13]—see Ref. [14] for details on this. Like previous works (e.g., Ref. [13]), we find that elastic processes are important for the computation of R_{AA}.

Our approach has the potential to reveal the effect of different soft-background models on hard observables. Figure 3 shows the result for R_{AA} using the $(2 + 1)$-dimensional hydrodynamic evolution from Refs. [38–40]. As initial temperatures are typically lower than in the $(3 + 1)$-dimensional hydro evolution, we need to increase α_s to 0.33 to describe the neutral pion R_{AA}. Further effects are demonstrated in the following section.

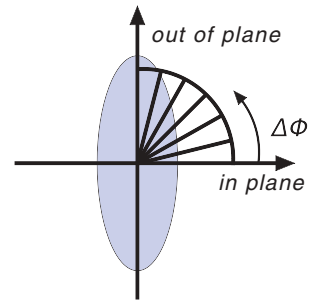

FIG. 4. (Color online) Binning in azimuth $\Delta\phi$ for the calculation of $R_{AA}(p_T, \Delta\phi)$ in noncentral collisions.

B. Angular dependence of the nuclear modification factor $\pi^0 R_{AA}(p_T, \Delta\phi)$

In Figs. 2 and 3, the neutral pion R_{AA} at midrapidity is averaged over the azimuthal angle with respect to the reaction plane ϕ. To learn more about the produced medium (e.g., to disentangle the effects of the density of the medium and the path length traversed on the energy loss), R_{AA} has been studied at midrapidity in *noncentral* collisions not only as a function of p_T but also as a function of the azimuth ϕ in Refs. [18–20]. We perform the same analysis within MARTINI and separate the azimuth in six bins of 15° each, reaching from 0° to 15° (in-plane) to 75° to 90° (out-of-plane), as shown in Fig. 4. R_{AA} is then determined in each bin separately. We employ both $(2 + 1)$- and $(3 + 1)$-dimensional hydrodynamic backgrounds and $\alpha_s = 0.33$ and $\alpha_s = 0.3$, respectively. Figure 5 shows the most extreme cases (0°–15° and 75°–90°) at $b = 7.5$ fm compared to recent midcentral (20–30%) data by PHENIX [20].

Particularly at lower p_T, we find a less pronounced difference between the in-plane and out-of-plane results than the data, as do previous theoretical calculations [19,55].

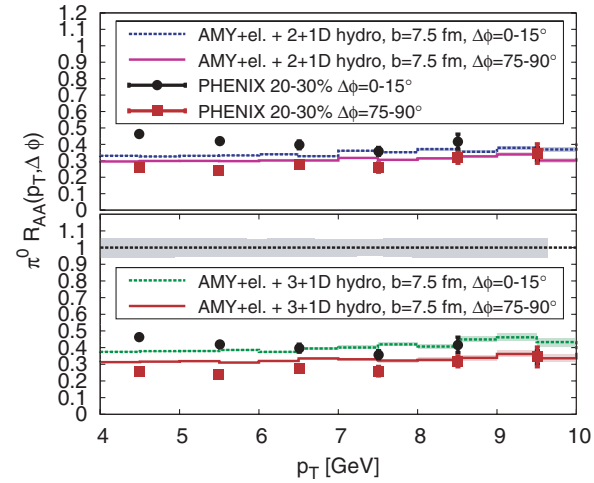

FIG. 5. (Color online) Nuclear modification factor as a function of p_T and $\Delta\phi$ for midcentral collisions at $\sqrt{s} = 200$ GeV. MARTINI results ($b = 7.5$ fm, upper panel $(2 + 1)$-dimensional hydro, $\alpha_s = 0.33$; lower panel $(3 + 1)$-dimensional hydro, $\alpha_s = 0.3$) with both radiative and elastic processes for most in-plane and most out-of-plane angular bins compared to PHENIX data from Ref. [20]. The gray band indicates the experimental error in R_{AA}.

Furthermore, one can see that the result is closer to the experimental data for the $(3+1)$-dimensional hydrodynamic background. This is due to a larger initial eccentricity in this case. Generally, we do not expect to describe the low p_T part correctly, because we do not incorporate soft physics such as flow effects or recombination. The too-small difference for $p_T \gtrsim 4$ GeV found in the simulation could stem in part from a too-small eccentricity of the initial state when using Glauber initial conditions in the hydrodynamic calculation or a too-large surface bias in the theoretical description. Use of color-glass-condensate initial conditions in $(3+1)$-dimensional hydrodynamics may help to improve the description of the data [56,57].

C. Photon production

Photons in the high p_T region produced in nuclear collisions are dominantly direct photons, fragmentation photons, and jet-plasma photons. Direct photons are included in PYTHIA. Apart from leading-order direct photons, PYTHIA produces additional photons emitted during the vacuum showers. Parts of these overlap with effects that are found in next-to-leading-order (NLO) calculations [58,59], but there is no simple theoretical way to identify the amount of overlap between the two. Also, fragmentation photons are part of the photons produced in the showers in PYTHIA. We computed photon production within PYTHIA with and without photons from showers and found that the shower contribution leads to an effective K factor of approximately 1.8 in the regarded p_T range.

For heavy-ion reactions, MARTINI adds the very relevant jet-medium photons from photon radiation $q \to q\gamma$ (bremsstrahlung photons) and jet-photon conversion via Compton and annihilation processes. As before, we include the full vacuum shower in the shown calculation—most of the shower photons will be emitted before the medium has formed and the parton has realized that it has formed. Improving on this approximation and including interference between vacuum and in-medium radiation will be the subjects of future work.

We present results for photon production in $p+p$ and Au + Au collisions at $\sqrt{s} = 200$ GeV compared to data by PHENIX [60–62] in Fig. 6.

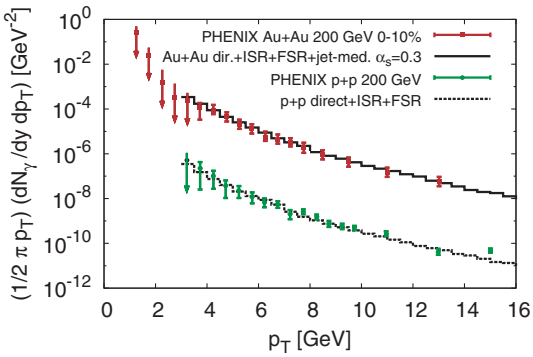

FIG. 6. (Color online) Photon yield in $p+p$ and Au + Au collisions at RHIC energy $\sqrt{s} = 200$ GeV. MARTINI results [$b = 2.4$ fm, $(3+1)$-dimensional hydro] compared to data from Refs. [60–62].

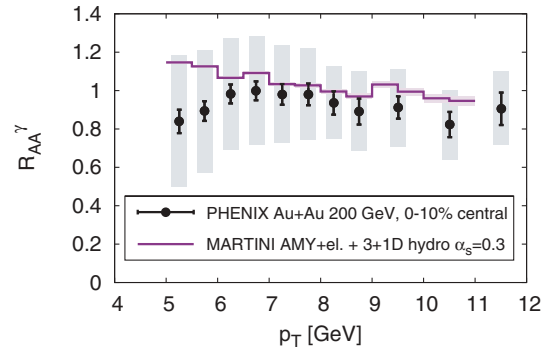

FIG. 7. (Color online) Photon nuclear modification factor for central collisions at $\sqrt{s} = 200$ GeV. MARTINI results are compared to data from Ref. [62]. See main text for details.

Another observable that provides information on the effect of the nuclear medium on photon production is the photon nuclear modification factor,

$$R_{\mathrm{AA}}^{\gamma} = \frac{1}{N_{\mathrm{coll}}(b)} \frac{dN_{\mathrm{AA}}^{\gamma}(b)/d^2p_T\,dy}{dN_{\mathrm{pp}}^{\gamma}/d^2p_T\,dy}. \tag{11}$$

Figure 7 shows R_{AA}^{γ} as a function of p_T for most central Au + Au collisions ($b = 2.4$ fm) at RHIC compared with 0–10% central PHENIX data. We find that in the approximation, including all photons from the vacuum shower leads to good agreement with the data within the error bars. Not including any photons from the final-state vacuum shower before τ_0, which corresponds to a pre-equilibrium contribution, reduces R_{AA} by approximately 20%.

V. CONCLUSIONS AND OUTLOOK

We present the first results obtained with the newly developed modular algorithm for relativistic treatment of heavy ion interactions (MARTINI). This hybrid approach describes the soft-background medium using hydrodynamics or other medium models and simulates the hard event microscopically, using PYTHIA 8.1 to generate individual hard nucleon-nucleon collisions. Hard partons are evolved through the medium using the McGill-AMY evolution scheme including radiative and elastic processes. Fragmentation is performed employing PYTHIA 8.1, which uses the Lund string fragmentation model. Apart from parameters in PYTHIA that were fixed by matching the neutral pion and photon spectra in $p+p$ collisons to experimental data, α_s is the only free parameter. Employing the $(3+1)$-dimensional hydrodynamic evolution from Ref. [41], we set it to $\alpha_s = 0.3$ to match the neutral pion R_{AA} measurement for central collisions. Using the same value for all other calculations (there was no additional freedom in any of the calculations), we were able to describe the neutral pion R_{AA} in midcentral collisions as well as photon yields and photon R_{AA}. For photon production, we added photons from jet-medium interactions to the prompt and shower photons that PYTHIA produces.

We have demonstrated that MARTINI is able to reveal the effect of using different evolution models for the soft background on results for hard observables. For example,

when using a $(2+1)$-dimensional hydrodynamical evolution model [38–40], a slightly different value for α_s ($\alpha_s = 0.33$) had to be employed to describe the experimental data. The calculated azimuthal dependence of the neutral pion $R_{\rm AA}$ in midcentral collisions turned out to be weaker than that found by PHENIX, for both shown hydrodynamic models, but more so for the $(2+1)$-dimensional one. This is mainly due to a larger initial eccentricity in the $(3+1)$-dimensional model. The result for the $(3+1)$-dimensional hydrodynamic background is along the line with previous calculations using different energy-loss schemes [19,55]. The weak azimuthal dependence, particularly for $p_T \lesssim 6$ GeV, can be due to the lack of soft-physics effects, such as flow and recombination, as well as a too-small eccentricity of the initial state when using Glauber initial conditions for the hydro-evolution calculation.

Having shown that MARTINI can reproduce one-body observables in good agreement with the data, the next step is to explore its full potential by studying many-body observables and correlations. Another future task is the implementation of heavy-quark evolution.

ACKNOWLEDGMENTS

We are happy to thank Steffen Bass, Evan Frodermann, Ulrich Heinz, Scott Moreland, Chiho Nonaka, and Huichao Song for very useful correspondence. We thank Torbjörn Sjöstrand for very helpful clarifications regarding PYTHIA 8.1 and gratefully acknowledge fruitful discussions with Guy Moore, Guang-You Qin, Thorsten Renk, Michael Strickland, and Vasile Topor-Pop. This work was supported in part by the Natural Sciences and Engineering Research Council of Canada. B.S. gratefully acknowledges a Richard H. Tomlinson grant by McGill University.

[1] A. B. Migdal, Phys. Rev. **103**, 1811 (1956).
[2] R. Baier, Y. L. Dokshitzer, A. H. Mueller, S. Peigne, and D. Schiff, Nucl. Phys. **B483**, 291 (1997).
[3] A. Kovner and U. A. Wiedemann (2003), arXiv:hep-ph/0304151.
[4] B. G. Zakharov, JETP Lett. **63**, 952 (1996).
[5] M. Gyulassy, P. Levai, and I. Vitev, Nucl. Phys. **B594**, 371 (2001).
[6] X.-N. Wang and X.-F. Guo, Nucl. Phys. **A696**, 788 (2001).
[7] B.-W. Zhang and X.-N. Wang, Nucl. Phys. **A720**, 429 (2003).
[8] A. Majumder, E. Wang, and X.-N. Wang, Phys. Rev. Lett. **99**, 152301 (2007).
[9] A. Majumder and B. Muller, Phys. Rev. C **77**, 054903 (2008).
[10] P. Arnold, G. D. Moore, and L. G. Yaffe, J. High Energy Phys. 12 (2001) 009.
[11] P. Arnold, G. D. Moore, and L. G. Yaffe, J. High Energy Phys. 11 (2001) 057.
[12] P. Arnold, G. D. Moore, and L. G. Yaffe, J. High Energy Phys. 06 (2002) 030.
[13] G.-Y. Qin, J. Ruppert, C. Gale, S. Jeon, G. D. Moore, and M. G. Mustafa, Phys. Rev. Lett. **100**, 072301 (2008).
[14] B. Schenke, C. Gale, and G.-Y. Qin, Phys. Rev. C **79**, 054908 (2009).
[15] S. A. Bass, C. Gale, A. Majumder, C. Nonaka, G. Y. Qin, T. Renk, and J. Ruppert, Phys. Rev. C **79**, 024901 (2009).
[16] T. Renk, Phys. Rev. C **74**, 034906 (2006).
[17] A. Majumder, Phys. Rev. C **75**, 021901(R) (2007).
[18] S. S. Adler *et al.* (PHENIX Collaboration), Phys. Rev. C **76**, 034904 (2007).
[19] R. Wei (PHENIX Collaboration) (2009), arXiv:0907.0024.
[20] S. Afanasiev *et al.* (PHENIX Collaboration) (2009), arXiv:0903.4886.
[21] S. Turbide, C. Gale, S. Jeon, and G. D. Moore, Phys. Rev. C **72**, 014906 (2005).
[22] S. Turbide, C. Gale, E. Frodermann, and U. Heinz, Phys. Rev. C **77**, 024909 (2008).
[23] G.-Y. Qin, J. Ruppert, C. Gale, S. Jeon, and G. D. Moore (2009), arXiv:0906.3280.
[24] R. J. Fries, B. Muller, and D. K. Srivastava, Phys. Rev. Lett. **90**, 132301 (2003).
[25] G.-Y. Qin, J. Ruppert, S. Turbide, C. Gale, C. Nonaka, and S. A. Bass, Phys. Rev. C **76**, 064907 (2007).
[26] T. Sjöstrand, S. Mrenna, and P. Skands, Comput. Phys. Commun. **178**, 852 (2008).
[27] T. Sjöstrand, S. Mrenna, and P. Skands, J. High Energy Phys. 05 (2006) 026.
[28] X.-N. Wang and M. Gyulassy, Phys. Rev. D **44**, 3501 (1991).
[29] A. Dainese, C. Loizides, and G. Paic, Eur. Phys. J. C **38**, 461 (2005).
[30] I. P. Lokhtin and A. M. Snigirev, Eur. Phys. J. C **45**, 211 (2006).
[31] I. P. Lokhtin *et al.*, Comput. Phys. Commun. **180**, 779 (2009).
[32] S. Wicks (2008), arXiv:0804.4704.
[33] T. Renk, Phys. Rev. C **78**, 034908 (2008).
[34] T. Renk (2008), arXiv:0808.1803.
[35] K. Zapp, G. Ingelman, J. Rathsman, J. Stachel, and U. A. Wiedemann, Eur. Phys. J. C **60**, 617 (2009).
[36] N. Armesto, L. Cunqueiro, and C. A. Salgado, Eur. Phys. J. C **63**, 679 (2009).
[37] K. J. Eskola, H. Honkanen, H. Niemi, P. V. Ruuskanen, and S. S. Rasanen, Phys. Rev. C **72**, 044904 (2005).
[38] P. F. Kolb, J. Sollfrank, and U. W. Heinz, Phys. Rev. C **62**, 054909 (2000).
[39] P. F. Kolb and R. Rapp, Phys. Rev. C **67**, 044903 (2003).
[40] P. F. Kolb and U. W. Heinz (2003), nucl-th/0305084.
[41] C. Nonaka and S. A. Bass, Phys. Rev. C **75**, 014902 (2007).
[42] U. W. Heinz, J. S. Moreland, and H. Song (2009), arXiv:0908.2617.
[43] S. Jeon and G. D. Moore, Phys. Rev. C **71**, 034901 (2005).
[44] P. Aurenche, F. Gelis, and H. Zaraket, J. High Energy Phys. 05 (2002) 043.
[45] M. Djordjevic, Phys. Rev. C **74**, 064907 (2006).
[46] C. W. De Jager, H. De Vries, and C. De Vries, At. Data Nucl. Data Tables **14**, 479 (1974).
[47] M. R. Whalley, D. Bourilkov, and R. C. Group (2005), hep-ph/0508110.
[48] K. J. Eskola, V. J. Kolhinen, and C. A. Salgado, Eur. Phys. J. C **9**, 61 (1999).

[49] K. J. Eskola, H. Paukkunen, and C. A. Salgado, J. High Energy Phys. 07 (2008) 102.
[50] K. Boyle (2005), http://www.phenix.bnl.gov/WWW/plots/search_plots.php?editkey=p0439.
[51] B. Andersson, G. Gustafson, G. Ingelman, and T. Sjostrand, Phys. Rep. **97**, 31 (1983).
[52] T. Sjostrand, Nucl. Phys. **B248**, 469 (1984).
[53] H. L. Lai *et al.* (CTEQ Collaboration), Eur. Phys. J. C **12**, 375 (2000).
[54] A. Adare *et al.* (PHENIX Collaboration), Phys. Rev. Lett. **101**, 232301 (2008).
[55] G.-Y. Qin, J. Ruppert, S. Turbide, C. Gale, C. Nonaka, and S. A. Bass, Phys. Rev. C **76**, 064907 (2007).
[56] T. Hirano, U. W. Heinz, D. Kharzeev, R. Lacey, and Y. Nara, Phys. Lett. **B636**, 299 (2006).
[57] A. Adil, H.-J. Drescher, A. Dumitru, A. Hayashigaki, and Y. Nara, Phys. Rev. C **74**, 044905 (2006).
[58] P. Aurenche, R. Baier, A. Douiri, M. Fontannaz, and D. Schiff, Nucl. Phys. **B286**, 553 (1987).
[59] P. Aurenche, R. Baier, M. Fontannaz, and D. Schiff, Nucl. Phys. **B297**, 661 (1988).
[60] S. S. Adler *et al.* (PHENIX Collaboration), Phys. Rev. Lett. **98**, 012002 (2007).
[61] A. Adare *et al.* (PHENIX Collaboration) (2008), arXiv:0804.4168.
[62] T. Isobe (PHENIX Collaboration), J. Phys. G **34**, S1015 (2007).